Please cite as: R. Aslam *et al.*, Smart Mater. Struct. (2016)**25**: 075036
DOI: 10.1088/0964-1726/25/7/075036

Magnetorheology of hybrid colloids obtained by spin-coating and classical rheometry

Raheema Aslam[1], Keshvad Shahrivar[2], Juan de Vicente[2] and Wenceslao González-Viñas[1]

[1] Dept. of Physics and Applied Mathematics, University of Navarra, Pamplona, Spain.
[2] Dept. of Applied Physics, University of Granada, Spain.

E-mail: wens@unav.es

Received 8 January 2016, revised 11 May 2016
Accepted for publication 19 May 2016
Published 16 June 2016

Abstract. Hybrid colloids composed of micron-sized ferromagnetic (carbonyl iron) and diamagnetic (silica) particles suspended in cyclohexanone, behave as, non-Newtonian, magnetorheological fluids. We measure and compare the magnetic field-dependent viscosity of hybrid diluted colloids using spin-coating and conventional magnetorheometry. We extend a previously developed model for simple colloids to this kind of hybrid colloids. As in the previous model, the viscosity of the colloidal suspension under applied fields can be derived from the surface coverage of the dry spin-coated deposits for each type of particles, and from the viscosity of the colloid at zero field. Also, our results allow us to obtain the evaporation rate of the solvent as a function of the rotation speed. Finally, we also measure the viscosity of the same suspension with a torsional parallel plate magnetorheometer under uniaxial DC magnetic fields aligned in the velocity gradient direction of a steady shearing flow. The experimental results under different conditions and the effect of each component on the magnetorheological properties of the resulting colloid are discussed. Standard spin-coating technique can be used both to characterize smart materials - complex fluids as well as to fabricate films with arbitrary solvents by tuning their viscosity by means of external fields.

PACS numbers: 83.85.cg, 47.15.gm, 47.65.-d

Keywords: magnetorheology, spin-coating, colloids

Accepted in: *Smart Mater. Struct.*

1. Introduction

Spin-coating technique has been used to make thin films on flat substrates for decades [1, 2, 3, 4, 5, 6, 7, 8, 9, 10, 11, 12, 13, 14, 15, 16]. It is very fast, reproducible, simple to perform and needs little material [17]. The thickness and the uniformity of the spin-coated films are important for the applications, and strongly dependent on the key parameters of the fluid such as viscosity, concentration, volume and evaporation rate as well as the process details (e.g. rotation speed, acceleration and time of spinning). Actually, the relevant phenomena that affect the spin-coating of complex fluids at different experimental conditions (e.g. the evaporation mechanism of the volatile solvent) remain unknown. To understand the spin-coating process, and to take from it the highest performance in applications, it is important to characterize the flow behavior as a function of the fluid properties. This has been studied through different models and experiments [2, 3, 5, 18, 19, 16, 20, 21]. Spin-coating of colloids has been thoroughly explored in the literature since the first half of twentieth century [1], specially in the case of nano-colloids for multiple applications in condensed matter. For colloids made of bigger particles, fine tuning in the experiments is much more relevant and not yet fully understood [22]. The use of external fields, as a way to tailor results, has only recently begun [23, 24, 25].

Pichumani *et al.* [23] used dilute suspensions of superparamagnetic particles for spin-coating experiments. They obtained sparse structures that consist of clusters of particles. On applying external magnetic fields during the spin-coating process, they observed an increase of the amount of the solids deposited on the substrate. After, they related the amount of deposit to the rheological properties of the colloid. Consequently, they were able to estimate the magnetoviscosity of the fluid [25] through a generalization of a continuum model [20] to a particulate system.

Traditionally, the magnetoviscosity of magnetic suspensions is measured using torsional rheometers that are conveniently adapted to apply external magnetic fields. In most cases, the suspensions are confined in between two parallel disks that are separated a commanded gap distance (typically between 100 microns and 1 mm). Then, a magnetic field is applied with the help of an electromagnet in the velocity gradient direction. This external magnetic field induces magnetic moments within the dispersed magnetizable particles that eventually interact through magnetostatic forces, promoting the formation of gap spanning elongated structures in the field direction. Hence, increasing the viscous dissipation and therefore the apparent viscosity under shearing flows. Interestingly, in practical applications particle loading and magnetic fields are generally large (above 10%(v/v) and 10 kA/m, respectively), and generate an apparent yield stress; a minimum stress level is required for the suspension to flow.

The influence of an external magnetic field in the rheological properties of magnetic suspensions and their applications (i.e. magnetorheology) has been studied extensively during the last half century [26, 27, 28, 29, 30, 31, 32, 33]. However, to date, there are several issues that are not fully understood yet. Undoubtedly, a hot topic today is the understanding of mixtures / hybrids suspensions. Experimental data [34, 35] and particle-level simulations [34] demonstrate a yield stress enhancement in certain hybrid suspensions prepared by partial substitution of magnetic microspheres by non-magnetic spheres [35, 36] and nanofibers [37]. Although it is clear that the sedimentation rate is related to the yield stress [38, 34, 35], a full explanation for the stress enhancement is still lacking in the literature.

A convenient way to get further information on the yielding and flow behavior of these suspensions involves the use of other complementary techniques such as ultrasounds [39] and spin-coating [23]. The latter is the subject of this work.

In this article, we extend our previous model [25] to hybrid colloids, to obtain the magnetoviscosity as a function of applied magnetic field, and the evaporation rate in spin-coating as a function of the rotation rate of the spinner. Here, we mix ferromagnetic particles and diamagnetic particles of different size, but of the same order of magnitude, in cyclohexanone. The surface coverage of the dried deposits obtained through spin-coating of the suspension, with and without magnetic fields, is measured. Firstly, we describe the experimental setup and procedures, then the considered previous models [20, 25] are outlined, and the one for the mixture is reported. Lastly, spin-coating results and those obtained from classical magnetorheometry are presented and discussed. The novel use of spin-coating technique [25] as a complement to conventional rheology is specially useful in the case of ill stabilized magnetorheological fluids. The spin-coating technique allows to measure in a very short time before the suspension destabilizes.

2. Experimental methods

In this work, we investigate a hybrid suspension prepared by dispersing carbonyl iron microparticles in cyclohexanone ($C_6H_{10}O$). The suspension also contains silica particles (SiO_2, ρ =1.8 g/cm^3, diameter $\approx$ 0.75 μm) that help to diminish a little bit the gravitational sedimentation of carbonyl iron particles during the

experiments. Recall that cyclohexanone physical properties (density: 947 kg/m^3, viscosity: 2.1 mPa·s) are similar to those of water.

Carbonyl iron powders used in the formulation were obtained by BASF SE (Germany) (grade EW), in which the Fe purity is greater than 96.8%. According to the manufacturer, their average diameter is $d_{50} \approx 3.0$ μm and their density is $\rho = 7.8$ g/cm^3. A very thin surface layer of silica exists, as demonstrated by XPS, that facilitates the re-dispersibility of these particles in suspension ([40] and references therein). The atomic concentration from XPS on the carbonyl iron particles used in this work is as follows: Fe 2p: 10.23%, O 1s: 44.94%, C 1s: 35.85%, and Si 2p: 8.98%.

Topographical images of the Long Wave Infra Red (LWIR, a.k.a. Thermal) emissivity are taken by a Xenics Gobi384, with an objective of microscope attached to it. These images allow us to distinguish clusters made of both kinds of particles in the deposits.

One set of experiments are performed in a customized commercial spin-coater (Laurell technologies, WS-650SZ-6NPP/LITE/OND) at rotation rates from 2000 to 7000 rpm. Applied magnetic fields ranging from 0 to 58.5 kA/m are generated by a pair of Helmholtz coils which are placed in such a way that the substrate spins in the region of uniform axial magnetic field. A sketch of the experimental setup is shown in Figure 1–C and photographs of the spin-coater and Helmholtz coils are shown in Figure 1–A and B. Applied magnetic fields are varied by adjusting the current in these coils with an external power supply.

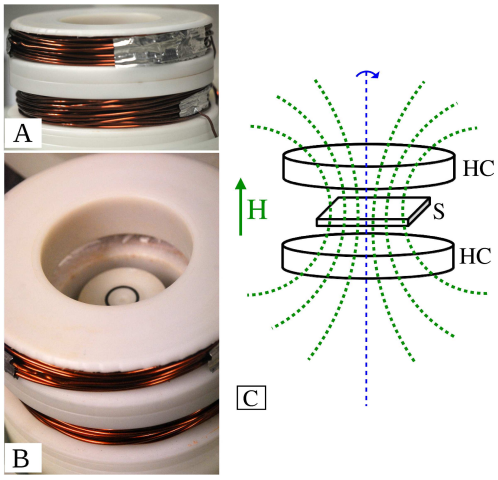

Figure 1. A and B – Photographs and schematics of experimental components: (A) A pair of Helmholtz coil and (B) mounted on spin-coater. (C) Sketch of experimental setup and the magnetic field lines (HC: Helmholtz coils; S: Substrate). The substrate spins in the region of uniform magnetic field. Reproduced from Ref. [25] with permission from the Royal Society of Chemistry.

The effective viscosity of the same suspension was determined at 25 °C using a MCR501 rheometer (Anton Paar, Germany) in plate-plate configuration (20 mm diameter, 300 microns gap). First, the samples were preconditioned at a constant shear rate (100 s^{-1}) during 20 seconds. Later, the plate was stopped and the field suddenly applied. This step allows the sample structuring. The final step consists in a stress log ramp from 0.102 Pa to 102 Pa still under external magnetic fields. The time interval employed to get every data within the full rheogram was 5 s. The external magnetic fields investigated ranged from 10 kA/m to 60 kA/m.

Glass substrates of an approximate size of 38 x 25 x 1 mm^3 are used for all experiments with the spin-coating technique. Firstly, they are cleaned with a diluted Micro-90 solution in an ultrasonic bath for fifteen minutes. Secondly, they are etched for forty minutes by a soft basic piranha, which consists of ultrapure water/ammonia/hydrogen peroxide with the ratio of 5:3:1 in volume at 67°C. Thirdly, the substrates are rinsed with ultra-pure water. Finally, they are dried by a filtered air blow. The clean substrates are then stored for 24 h before each experiment.

In the suspensions, we use the same mass of carbonyl iron particles and silica particles. They are weighed and homogeneously suspended in cyclohexanone to obtain a total particle concentration of 1.5% (v/v). The individual volume fractions are 0.003 (iron), 0.012 (silica), and 0.985 (cyclohexanone). The suspension is ultrasonicated for several hours and vigorously shaken before commencing the experiments to ensure a well-dispersed suspension. Additionally, before each experimental spin-coating process, the suspension is ultrasonicated for fifteen minutes and vigorously shaken. The spin-coater is operated at a required rotation rate ω and the external magnetic field H is applied. Then, 100 μl of suspension is pipetted onto the spinning substrate. Once the spun suspension is dried, the field is turned off. Micrographs are taken on the substrates at 2 mm intervals from the center of spinning. In a previous learning phase, we observed that deposits under identical conditions were very similar, leading to reproducible results within their experimental errors. Thus, we analyzed one micrograph for each set $\{\omega, H, r\}$, where r is the distance to the center of spinning to obtain the surface coverage by both kinds of particles (with reflected light microscopy). Also, we analyzed another micrograph for each set $\{\omega, H\}$ to obtain the surface coverage of carbonyl iron particles alone with LWIR microscopy. Typical micrographs are shown (figure 2) for experiments performed at 19.5 kA/m, 5000 rpm (Figure 2a-c), and at 48.7 kA/m, 2000 rpm (Figure 2d). The images are analyzed through home-made routines in Octave. As almost all the deposits from the experiment are submonolayers,

except some iron deposits when magnetoviscosity has been very high (Figure 2d), we characterize the amount of deposit by the area occupied by clusters of particles relative to the total area of the field of view. This value is measured for each micrograph and it is called the "occupation factor" or surface coverage ε^2.

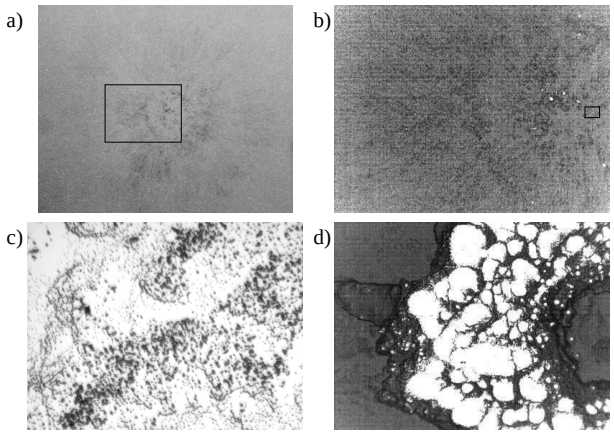

Figure 2. Micrographs of the deposits resulting from spin-coating with spinning rate 5000 rpm and applied magnetic field of 19.5 kA/m at different magnifications (a-c) and comparison with deposits obtained at 48.7 kA/m and 2000 rpm (d).
a) Transmission image of the center of the deposit at low magnification. Horizontal Field of View (HFOV) is 27.7 mm, and the rectangle shows the region that corresponds to b) Thermal camera image showing different emissivity. Here, carbonyl iron is very bright. HFOV=8.4 mm, and the small rectangle shows the region that corresponds to c) Reflected light image at the center of spinning. HFOV=0.66 mm. d) Thermal camera image with HFOV=8.4 mm. Here, also carbonyl iron is very bright, but its surface coverage is much larger than in (b). In all the cases, the overall concentration of the suspension is 1.5% (v/v), and the diameters of carbonyl iron and silica particles are 3 μm and 0.75 μm respectively.

Although elongated clusters clearly appear when a magnetic field is applied, in previous similar experiments it has been proved that they are not oriented [23], despite the axial symmetry in the system. This indicates that a symmetry breaking instability is taking part either for a diluted suspension, or for experiments where a magnetic field is applied.

The validity of the simple model for colloids has been previously checked [23, 25, 22] by comparing experiments with several different conditions to a reference one [41]. Consequently, in the present work we do not compare our results to any reference experiment, but considering valid the simple colloids model (outlined below) to extract conclusions.

3. Results and discussion

3.1. Models

3.1.1. Simple fluids model [20]. The original model by Cregan *et al.* [20] for spin-coating is based on the lubrication approximation and uses the matched asymptotic expansions technique to get a much better solution than the one obtained by Meyerhofer [3]. The most critical assumptions to utilize this model are the following: firstly, the evaporation rate of the solvent is taken as constant (i.e. it does not depend on the parameters of the experiment, like ω). Secondly, the fluid is considered as Newtonian and finally, the fluid is not a colloid in the sense that it is not a particulate system. One of their relevant results is the thickness (or height) of the deposited solute (not colloidal particles) as a function of some parameters of the suspension and of the spin-coating process (last equation of [20], which written in our notation corresponds to eq. 2 of [25]):

$$h_\infty^{(s)} = \frac{C}{1-C}\left(\frac{3}{2}\nu E\right)^{\frac{1}{3}}\omega^{-\frac{2}{3}}, \tag{1}$$

where $h_\infty^{(s)}$ is the final deposited film thickness, C is the initial concentration in v/v or volume fraction (in our experiments 0.015, or 1.5%), ω is the rotation rate, ν is the kinematic viscosity of the solvent, E is evaporation rate of solvent. To simplify notation it is possible to put eq. 1 as:

$$h_\infty^{(s)} \equiv A\omega^{-\beta}, \tag{2}$$

where A is a constant over the experiment and $\beta = \frac{2}{3}$.

3.1.2. Evaporation rate. Cregan's model assumes a constant evaporation rate through the whole process of spin-coating. However, evaporation rate depends on rotation rate and on parameters of the suspension and the experiment [3, 41]. Using the 'ansatz' that Cregan model is valid even in the cases where the evaporation rate is not constant, we can obtain the evaporation rate behavior at different conditions, by inverting eq. 1 for E:

$$E(\omega) = \left[\frac{1-C}{C}h_\infty^{(s)}\right]^3\frac{2\omega^2}{3\nu}. \tag{3}$$

3.1.3. Simple colloids model – magnetorheology by spin-coating [25]. In a particulate system (i.e. colloid), the effective local amount of solids deposited on the substrate (i.e. without taking the voids into account) depends on the kind of deposited structure (see Fig. 4 in [25] and the corresponding text) and is the packing fraction times the Voronoi cell [42] volume. We call as the compact equivalent height (CEH), the effective deposited volume per unit area. In short, wherever for simple fluids appear $h_\infty^{(s)}$ (e.g. in eqs. 1, 2 and 3), it has to be replaced by CEH for colloids. In consequence, eqs. 1 and 2 become:

$$\mathrm{CEH} = \frac{C}{1-C}\left(\frac{3}{2}\nu E\right)^{\frac{1}{3}}\omega^{-\frac{2}{3}}, \tag{4}$$

$$\mathrm{CEH} \equiv A\omega^{-\beta}. \tag{5}$$

Also, equation 4 can be generalized by including an evaporation rate that may depend on ω, but not on the magnetic field [25]. As a consequence, it is obtained in eq. 5 that $\beta \neq \frac{2}{3}$, and eq. 3 becomes:

$$E(\omega) = \left[\frac{1-C}{C}\mathrm{CEH}\right]^3 \frac{2\omega^2}{3\nu}. \tag{6}$$

In a submonolayer deposit with hexagonal structure (see section 3.2 in [25] for more details), which can be obtained through a diluted suspension:

$$\mathrm{CEH} = \frac{2\pi}{3\sqrt{3}} R \cdot \varepsilon^2, \tag{7}$$

where R is the radius of the particles and ε^2 is occupation factor, which is measured through imaging techniques as it has been previously explained.

Consequently, we have access to all parameters if the kinematic viscosity ν of the solvent and the radius R of the particles are known. Then, it is possible to effectively obtain the evaporation rate by means of eq. 6.

Using this model, Pichumani *et al.* [25] compared two experiments performed in the same conditions, except for the applied magnetic field, that lead to submonolayers. The comparison is made by computing the ratio of their corresponding CEH in the presence and absence of magnetic fields, using eq. 7:

$$\frac{\mathrm{CEH}(H,\omega)}{\mathrm{CEH}(H=0,\omega)} = \frac{\varepsilon^2(H,\omega)}{\varepsilon^2(H=0,\omega)}. \tag{8}$$

If we substitute the CEHs in the left hand side of equation 8 by the corresponding generalized Cregan equation (i.e. eq. 4), the only parameter which remains dependent on the field is the kinematic viscosity ν. This leads to [25]:

$$\frac{\nu(H,\omega)}{\nu(H=0,\omega)} = \left[\frac{\varepsilon^2(H,\omega)}{\varepsilon^2(H=0,\omega)}\right]^3. \tag{9}$$

3.1.4. Hybrid colloids model. In the case where there is more than one specie for the discrete phase (more than one kind of particles), it is possible to further generalize Cregan's equation by taking again into account that the equivalent spin-coated deposit (CEH) should behave similarly to that of a non-particulate system and equation 4 can be used. However, eq. 7 is:

$$\mathrm{CEH} = \frac{\pi}{3\sqrt{3}} \sum_i (2R_i) \cdot \varepsilon_i^2, \tag{10}$$

where subindex i refers to the kind of particle. Thus, eq. 8 becomes:

$$\frac{\mathrm{CEH}(H,\omega)}{\mathrm{CEH}(H=0,\omega)} = \frac{\sum_i (2R_i) \cdot \varepsilon_i^2\ (H,\omega)}{\sum_i (2R_i) \cdot \varepsilon_i^2 (H=0,\omega)}, \tag{11}$$

where the compact equivalent height follows the generalized Cregan's equation (eq. 4). Substituting, we obtain:

$$\frac{\nu(H,\omega)}{\nu(H=0,\omega)} = \left[\frac{\sum_i (2R_i) \cdot \varepsilon_i^2 (H,\omega)}{\sum_i (2R_i) \cdot \varepsilon_i^2 (H=0,\omega)}\right]^3. \tag{12}$$

Finally, as the occupation factor is approximately a conserved magnitude for same order of magnitude sized particles, we have that:

$$\varepsilon^2_{\mathrm{total}} \approx \sum_i \varepsilon_i^2. \tag{13}$$

3.2. Experimental results and discussion

Figure 3 shows the normalized viscosity of the magnetic suspension obtained by classical rheometry as a function of the applied magnetic field. When the magnetic field strength increases, for a given shear stress value, the normalized viscosity increases monotonically. Of course, by increasing the shear stresses, the normalized viscosity decreases as hydrodynamic forces overcome the magnetostatic ones, hence destroying the field-induced structures.

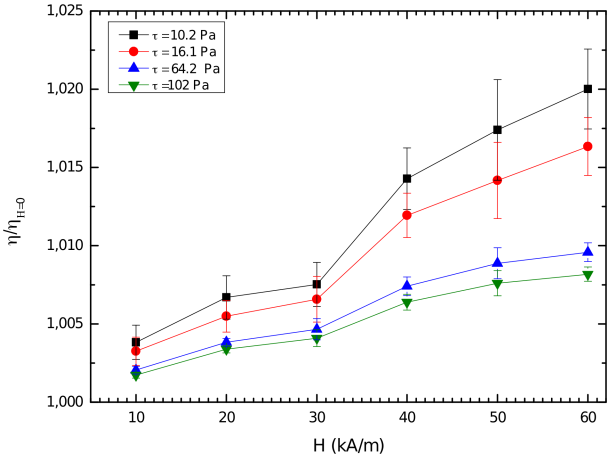

Figure 3. Normalized viscosity of the hybrid magnetorheological suspensions (concentration 1.5% (v/v), diameters of carbonyl iron and silica particles 3 μm and 0.75 μm, respectively) for several shear stress values, as a function of the magnetic magnetic field strength. Shear rate ranges from 60 to 650 [1/s] for data points corresponding to different shear stresses (from 10.2 Pa to 102 Pa). The particular shear rate value depends on the magnetic field.

Fig. 2c is a typical micrograph that allows us to obtain, from the surface coverage of the dried spin-coated deposits at a given distance from the center of rotation, the total occupation factor $\varepsilon^2_{\mathrm{total}}$ (total area occupied by both kinds of particles divided by the total substrate area). Fig. 2b is an example of the thermal micrographs that allow us to obtain

the occupation factor for carbonyl iron particles $\varepsilon^2_{\mathrm{Fe}}$. Occupation factor of silica can be easily obtained from $\varepsilon^2_{\mathrm{total}} \approx \varepsilon^2_{\mathrm{Fe}} + \varepsilon^2_{\mathrm{SiO_2}}$

Due to the particulate nature of the solute, the raw measured occupation factors can be translated into the compact equivalent height (eqs. 10, 13). See fig. 4.

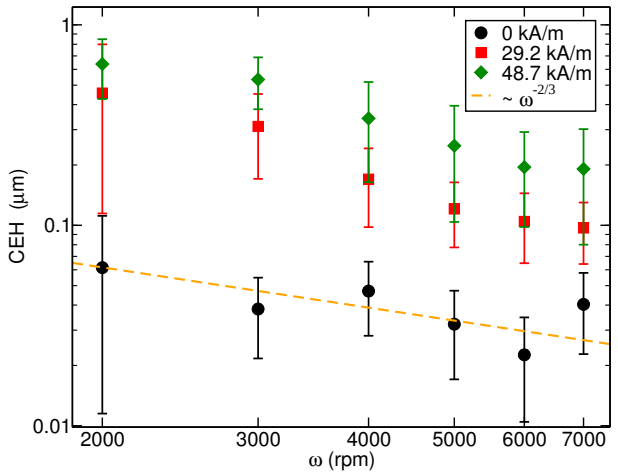

Figure 4. Compact equivalent height (CEH) without and with applied magnetic fields. For the mixture of SiO_2 and carbonyl iron suspension in cyclohexanone of concentration of 1.5% (v/v) and diameters of carbonyl iron and silica particles 3 μm and 0.75 μm, respectively: black circles at H= 0 kA/m; squares at H= 29.2 kA/m; diamonds at H= 48.7 kA/m. Dashed line is a fit to the power law from the Cregan's model [20].

The correspondence between circles (CEH from the experimental data) and dashed line (power law from Cregan's model) in fig. 4 shows that Cregan's generalized model also holds for our system at zero-field. We also investigate the dependence of evaporation rate on the rotation speed. Using eqs. 6, 10 and 13, we obtain fig. 5, which shows that, evaporation rate is approximately constant except for higher ω, in agreement with Cregan's generalized model.

The qualitative change in evaporation rate at high rotation rates may be due to the change in the mechanisms involved in the removal of the solvent vapor from the boundary layer to the atmosphere, and in the filtration of the liquid solvent through the colloidal particles to reach the colloid surface [3, 43, 4]. If the rotation rate is taken as the control parameter, a bifurcation appears which interchanges the relevant mechanism in the considered range of rotation rates [44, 45]. The order of magnitude of the evaporation rates ($\sim$1 μm/s) in our experiments is in agreement with previous literature [46].

Using eqs. 12 and 13, we obtain figure 6. There, we can observe a very high effective magnetoviscosity for low shear rates (frequencies of rotation). In those cases, there is phase separation, allowing a faster evaporation and a much more compact deposition (e.g. fig. 2d). Although a monotonic decrease of the

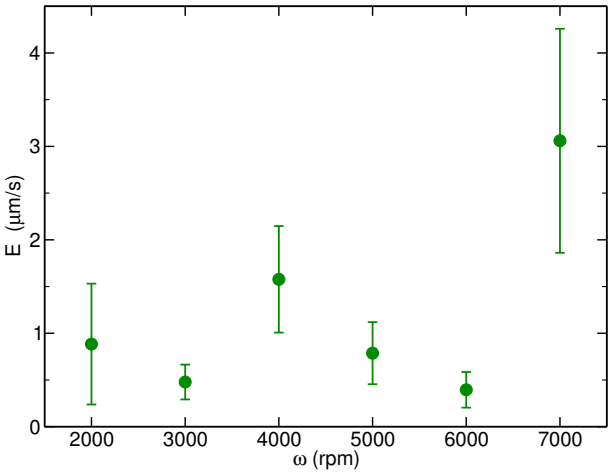

Figure 5. Effective evaporation rate as a function of the frequency of rotation, for the case of zero-field and concentration 1.5% (v/v), and diameters of carbonyl iron and silica particles 3 μm and 0.75 μm, respectively.

normalized viscosity is almost within the experimental error, we think that the apparent increase of viscosity at 3000 rpm is worth to be further investigated in order to either define a new dynamical regime or rule it out.

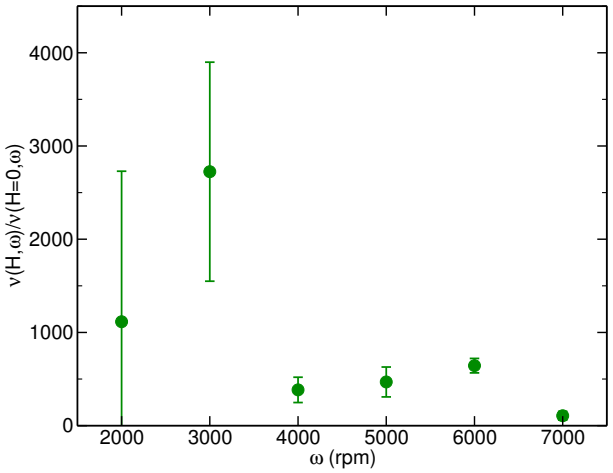

Figure 6. Normalized effective magnetoviscosity at 48.7 kA/m. Concentration of the suspension is 1.5% (v/v), and the diameters of carbonyl iron and silica particles are 3 μm and 0.75 μm respectively.

As a matter of fact, when a magnetic field is applied to a diluted magnetorheological fluid, chains of colloidal particles are formed [47, 48], which increase the effective viscosity of the colloid. At high enough shear stresses those chains break diminishing the effective viscosity. Thus, the colloid under applied magnetic field behaves as a shear-thinning non-Newtonian fluid.

Averaging $\frac{\nu(H,\omega)}{\nu(H=0,\omega)}$ over ω for a range of magnetic field strengths we obtain fig. 7. A large

magnetoviscosity increase can be observed similarly to measurements in other magnetorheological fluids [49]. Large error bars could be due to the large non-Newtonian character of the colloid under magnetic fields.

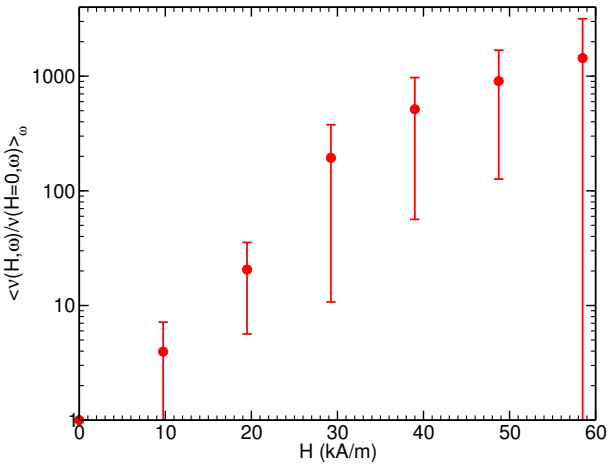

Figure 7. Average normalized magnetoviscosity as a function of applied field. Error bars correspond to the variability of normalized viscosity as a function of rotation rate. The concentration of the suspension is 1.5% (v/v), and the diameters of carbonyl iron and silica particles are 3 μm and 0.75 μm respectively.

We now compare the magnetorheological results obtained from the two different techniques in hybrid colloids of the same concentration, from fig. 3 (classical rheometry) and fig. 7 (spin-coating). We observe that the change in the relative viscosity from classical rheometry is much smaller than the one from spin-coating. Although the presence of silica particles was intended to reduce the sedimentation rate, the characteristic time of sedimentation is smaller than the time needed to proceed with the classical rheometry experiment. This causes a heterogeneous stratification in the colloid that reduces the effective viscosity. As a result, there is an upper region very diluted of magnetic particles, which are mostly sedimented below. Only few magnetic particles held by the presence of silica particles in the suspension may contribute to the measurements. A similar observation was recently reported by carefully conducted experiments using a QCM [50]. Therefore, we observe a small change in the normalized viscosity (see fig. 3). Further, spin-coating experiments are performed within an elapsed time where the magnetic particles in the suspension barely sediment. Hence, magnetic particles are homogeneously distributed in the suspension and they all contribute to the final change in the relative viscosity (see fig. 7). From the comparison we anticipate that, it is possible to study magnetorheology and the non-Newtonian character of diluted hybrid colloids by spin-coating. On the one hand, this technique could be more efficient than the classical rheometry to study rheology of dilute colloids made of very big particles in volatile solvents. On the other hand, classical rheometry is much better for dealing with nano-colloids or when used with non-volatile solvents, where rheometry by spin-coating is not useful.

4. Summary and concluding remarks

The change in the magnetic field-dependent viscosity of diluted magnetic suspensions is obtained using two different techniques: classical rheometry and spin-coating. We show that the rheology of hybrid colloids in volatile solvents can be characterized by spin-coating. Also, we obtain the effective rotation speed dependent evaporation rate that is almost constant in the range of our experimental conditions and, thus, consistent with the generalized Cregan's equation (eq. 5) with exponent $\beta = \frac{2}{3}$. It is worth to mention that this evaporation rate is much higher than the static absolute evaporation rate of cyclohexanone. However, it is of the order of magnitude obtained previously [46]. Moreover, its relative value to other solvents during spin-coating is in agreement with the expected value.

Comparison of spin-coating results with those obtained from established rheological tools [33] suggests that classical rheometry can be employed but the presence of sedimentation during the measurement is challenging in dilute systems. Spin-coating technique provides faster experiments and hence sedimentation is not critical.

Although we have proved the main effect of applied magnetic fields in colloidal spin-coating, further research has to be done to clarify the dynamics of each of the components of the suspension, that give rise to the observed patterns. Also, it remains not clear what would be the microstructure in more concentrated suspensions. Nevertheless, we anticipate that the generalized model could be used in that case, as we know that it worked for the case of non-magnetic colloidal suspensions (see e.g. [25]); thus, only changing the effective evaporation rate. For the same reason, we think that a different proportion in volume fractions of silica and carbonyl iron particles will only change the evaporation rate as well as the values of other parameters from the model. We should note that in those cases, classical rheometry methods are useful, too.

The technique we proved that works to extract, from experimental results, the rheological properties of hybrid colloids under different conditions (i.e., external fields), not only is useful for smart materials such as magnetorheological fluids in an applied mag-

netic field, but also could be used for electrorheological fluids [51] under electric fields and suspensions without any applied field [52]. It is specially interesting for fluids, where sedimentation is comparable or more important than interparticle interactions (hydrodynamic, magnetic, ...), where other techniques cannot be utilized easily. Spin-coating technique is used traditionally to fabricate films on substrates. This work opens the possibility of tailoring the morphology of deposited smart materials, by fine tuning the viscosity of the spun suspensions with the help of an external field.

It is also important to remark that in the field of smart materials this work opens possibility to fabricate and characterize new materials at short time-scales and/or in film form, which can neither be studied nor obtained for long times and in bulk form by means of traditional rheometry or other classical techniques.

Acknowledgments

This work was partly supported by the Spanish MINECO (Grants n. FIS2014-54101-P, MAT2013-44429-R, PCIN-2015-051) and Junta de Andalucía (Grants n. P10-RNM-6630 and P11-FQM-7074). RA acknowledges financial support from the "Asociación de Amigos de la Universidad de Navarra".

References

[1] Walker P H and Thompson J G 1922 *P. Am. Soc. Test. Mater.* **22** 465
[2] Emslie A G, Bonner F T and Peck L G 1958 *J. Appl. Phys.* **29** 858–862
[3] Meyerhofer D 1978 *J. Appl. Phys.* **49** 3993–3997
[4] Rehg T J and Higgins B G 1992 *AIChE J.* **38** 489
[5] Birnie III D and Manley M 1997 *Phys. Fluids* **9** 870–875
[6] Acrivos A, Shah M J and Petersen E E 1960 *J. Appl. Phys* **31** 963
[7] Wahal S, Oztekin A, Bornside D, Brown R, Seidel P, Ackmann P and Geyling F 1993 *Appl. Phys. Lett.* **62** 2584
[8] Furukawa H, Tsutsui H, Aoi K, Watanabe T and Nakamura I 2005 *J. Phys.: Conference Series* **14** 220–227
[9] Bornside D E, Macosko C W and Scriven L E 1989 *J. Appl. Phys.* **66** 5185–5193
[10] Hall D, Underhill P and Torkelson J 1998 *Polym. Eng. Sci.* **38** 2039–2045
[11] Fraysse N and Homsy G M 1994 *Phys. Fluids* **6** 1491
[12] Ohara T, Matsumoto Y and Ohashi H 1989 *Phys. Fluids A* **1** 1949
[13] Mihi A, Ocaña M and Míguez H 2006 *Adv. Mater.* **18** 2244–2249
[14] Sahu N, Parija B and Panigrahi S 2009 *Indian Journal of Physics* **83** 493–502
[15] Arcos Martínez C 2008 *Preparación y Caracterización de Materiales Mesoestructurados* Ph.D. thesis Facultad de Ciencias, Universidad de Navarra
[16] Giuliani M 2010 *Colloidal crystal formation through interfacial mechanisms* Ph.D. thesis Facultad de Ciencias, University of Navarra
[17] Wu Y L 2007 *Control over colloidal crystallization by shear and electric fields* Ph.D. thesis Utrecht University
[18] Higgins B G 1986 *Phys. Fluids* **29** 3522
[19] Zhao Y and Marshall J 2008 *Phys. Fluids* **20** 043302
[20] Cregan V and O'Brien S 2007 *J. Colloid Interf. Sci.* **314** 324
[21] Cregan V and O'Brien S B 2013 *Applied Mathematics and Computation* **223** 76–87
[22] Pichumani M, Bagheri P, Poduska K M, González-Viñas W and Yethiraj A 2013 *Soft Matter* **9** 3220–3229
[23] Pichumani M and González-Viñas W 2011 *Magnetohydrodynamics* **47** 191
[24] Bartlett A P, Pichumani M, Giuliani M, González-Viñas W and Yethiraj A 2012 *Langmuir* **28** 3067
[25] Pichumani M and González-Viñas W 2013 *Soft Matter* **9** 2506–2511
[26] Jolly M R, Carlson J D and Muoz B C 1996 *Smart Materials and Structures* **5** 607
[27] Parthasarathy M and Klingenberg D 1996 *Mater. Sci. Eng. R-Reports* **17** 57–103
[28] Dyke S J, Spencer Jr B F, Sain M K and Carlson J D 1998 *Smart Materials and Structures* **7** 693
[29] Ginder J 1998 *MRS Bulletin* **23** 26–29
[30] Olabi A and Grunwald A 2007 *Materials and Design* **28** 2658–2664
[31] Vekas L 2008 *Advances in science and technology* **54** 127–136
[32] Park B J, Fang F F and Choi H J 2010 *Soft Matter* **6** 5246–5253
[33] de Vicente J, Klingenberg D and Hidalgo-Alvarez R 2011 *Soft Matter* **7** 3701–3710
[34] Ulicny J C, Snavely K S, Golden M A and Klingenberg D J 2010 *Applied Physics Letters* **96** 231903
[35] Powell L A, Wereley N M and Ulicny J 2012 *IEEE Transactions on Magnetics* **48** 3764–3767
[36] Ohori S, Fujisawa K, Kawai M and Misumata T 2013 *Chem. Lett.* **42** 50–51
[37] Bombard A, Gonçalves F, Morillas J and de Vicente J 2014 *Smart Mater. Struct.* **23** 125013
[38] Ngatu G T and Wereley N M 2007 *IEEE Transactions on Magnetics* **43** 2474–2476
[39] Rodríguez-López J, Elvira L, de Espinosa Freijo F M, Bossis G and de Vicente J 2013 *Appl. Phys. Lett.* **102** 081907
[40] Bombard A, Gonçalves F, Shahrivar K, Ortiz A and de Vicente J 2015 *Tribology International* **81** 309–320
[41] Giuliani M, González-Viñas W, Poduska K M and Yethiraj A 2010 *J. Phys. Chem. Lett.* **1** 1481–1486
[42] Voronoi G 1908 *J. reine angew. Math.* **134** 198–287
[43] Skrobis K J, Denton D D and Skrobis A V 1990 *Polymer Engineering & Science* **30** 193–196
[44] Bornside D E, Brown R A, Ackmann P W, Frank J R, Tryba A A and Geyling F T 1993 *J. Appl. Phys.* **73** 585–600
[45] Öztekin A, Bornside D E, Brown R A and Seidel P K 1995 *J. Appl. Phys.* **77** 2297–2308
[46] Larson R G and Rehg T J 1997 *Liquid Film Coating* (Springer) chap Spin coating, pp 709–734
[47] Melle S, Fuller G G and Rubio M A 2000 *Phys. Rev. E* **61** 4111
[48] Melle S, Rubio M and Fuller G 2001 *Int. J. Mod. Phys. B* **15** 758–766
[49] Shah K and Choi S B 2014 *Front. Mater.* **1** 21
[50] Rodríguez-López J, Castro P, de Vicente J, Johannsmann D, Elvira L, Morillas J and de Espinosa F M 2015 *Sensors* **15** 30443–30456
[51] Stanway R, Sproston J L and El-Wahed A K 1996 *Smart Materials and Structures* **5** 464
[52] Ederth J, Hultaker A, Heszler P, Niklasson G A, Granqvist C G, van Doorn A K J, van Haag C, Jongerius M J and Burgard D 2001 Electrical and optical properties of thin films prepared by spin coating a dispersion of nano-sized tin-doped indium-oxide particles vol 4590 pp 280–285